Fully Automated, MRI-based Left-Ventricular Contractility Analysis in Breast Cancer Patients Following Chemotherapy

Bryant M. Baldwin, Gaelyn V. Angus-Barker, Shane Joseph, Maria S. Figarola, Michael V. Cohen,
Christopher M. Malozzi and Julia Kar
University of South Alabama, Mobile, Alabama, USA
bmb1523@jagmail.southalabama.edu

Abstract— This study investigated if measurements of mechanical contractile parameters, such as strains, torsion and left-ventricular ejection fraction (LVEF), are indicative of left-ventricular (LV) remodeling that may occur in patients who have been exposed to the anthracycline and trastuzumab type of chemotherapeutic agents (CA). An equally important goal was investigating this contractility using a single-scan cardiac strain analysis tool comprising of the Displacement Encoding with Stimulated Echoes (DENSE) sequence for MRI scans and the Radial Point Interpolation Method (RPIM). Data was acquired in 11 patients who had been exposed to CA agents and were under either a regimen of breast cancer antineoplastic drugs and/or were being treated for cardiac complications. A Bland-Altman analysis of interobserver strain measurements showed agreements of 0.01 ± 0.06 for longitudinal strain, $0.10 \pm 1.92°$ for torsion. Enlarging of the LV in the patient population was indicated by a significant difference in their diastolic diameters in healthy subjects. Significant longitudinal strains differences were seen between patients and healthy subjects which were 0.15 ± 0.03 vs 0.21 ± 0.04 (p=0.02) and 0.17 ± 0.02 vs 0.22 ± 0.03 (p=0.01) for the mid-ventricular and apical sections. A similar result for torsion was found between patients and healthy subjects for the mid-ventricular and basal sub-regions. The results from the statistical analysis show the likelihood of LV remodeling and fibrosis in these patients that is otherwise not indicated by LVEF measurements.

I. INTRODUCTION

The administration of certain anti-neoplastic chemotherapeutic agents (CA), such as anthracyclines and trastuzumab, in breast cancer patients may lead to the complications of developing cardiotoxicity, and counter any gains in survivorship achieved with this form of treatment [1-6]. The cardiotoxicity-based dysfunctions caused by CAs that range from arrhythmias to irreversible heart failure require robust and managed care, such as guideline directed medical therapy (GDMT), that ensures patient longevity [7]. Hence, chemotherapy treatment plans and those related to cardiotoxicity induced by it should incorporate surveillance measures consisting of routine monitoring of left-ventricular (LV) contractility, which can effectively prevent the onset of irreversible damage or lower the incidence of heart failure [1, 3, 8-15]. To this effect, scientific evidence and a growing number of clinical studies show that a most effective way of monitoring contractile pattern changes is via computations of LV myocardial strain, a metric of contractile function that has been proven to be a more sensitive biomarker for detecting cardiotoxicity than dysfunction measured via reductions in left ventricular ejection fraction (LVEF) [13, 16-18]. This study was conducted to investigate the feasibility of a fully automated, single-scan, MRI-based methodology for assessing LV chamber quantifications and 3D strain toward predicting any cardiac remodeling that may occur in survivors of breast cancer who have undergone CA-based cardiotoxicity [4, 10, 15, 16, 19]. Of particular note is that this study specifically targeted the computation of LV twists and torsions (in addition to 3D strain) given a prevailing belief in the scientific community that any abnormal torsion indicates the altered wringing motions in the heart's myofibers during ejection, and is a major indicator of cardiac dysfunction [20-22]. The detection algorithm consists of a novel, automated 3D methodology that rapidly tracks LV boundary motion and analyzes 3D strain following phase unwrapping of MRI data obtained with the navigator-gated spiral Displacement Encoding with Stimulated Echoes (DENSE) sequence [23-32]. Additionally, this analysis technique is also capable of generating 3D surface strain maps in all six independent strain directions. The possibility of cardiac remodeling and occurrence of LV dysfunction was tested on MRI DENSE data acquired in eleven breast cancer survivors who had undergone CA-based chemotherapy and were under either a regimen of managed care for cardiac complications and/or continued breast cancer therapy.

II. EXPERIMENTAL DESIGN

A. Human Subject Recruitments

Eleven breast cancer patients who had previously undergone chemotherapeutic treatment were imaged in a 1.5 Tesla Espree (Siemens, Erlangen, Germany) MRI scanner using the navigator-gated 3D Spiral DENSE sequence [26, 27]. All subjects (including healthy) signed informed consents in accordance with the university's Institutional Review Board (IRB) guidelines and who volunteered access to their breast cancer and cardiac treatment plans for the purposes of this study.

The patients had undergone CTA-based (anthracyclines and trastuzumab) chemotherapy and were under

continued surveillance and some under a regimen of managed care for non-acute cardiac complications related to cardiotoxicity (rated at NYHA class = II or less). To rule out the effects of acute comorbidity influencing the results of LV strains from cardiotoxicity, the exclusion criteria for patients included LVEF less than 50%, valvular heart disease, ischemic heart disease and acute infarction, severe hypertension and a terminal life expectancy of fewer than 3 months. Overall, a preserved, TTE-measured LVEF higher than 50% at the inception of chemotherapy was the most important criteria for recruitment. Due to the likelihood of developing common cardiac side-effects following chemotherapy, patients were not excluded if they had developed non-acute conditions that often follow CTA-based chemotherapy, such as arrhythmias without atrial or ventricular fibrillation and hypertension [15, 19]. Hence, patients who had developed post-chemotherapy comorbidities rated above NYHA class II were not included. The timeline for recruiting patients was within 12 months from the end of their chemotherapy such that strain analysis was conducted when the most clinically relevant form of cardiotoxicity occurs [10, 15]. The MRI study in each patient was scheduled within a 3 days window following a post-chemotherapy TTE exam to ensure the patient's DENSE and TTE-based LVEFs were comparable. Patients were consecutively recruited following their cardiologist's referral, given they met the above cardiac risk criteria and had completed their post-chemotherapy TTE. The CTA treatment each patient underwent was either one of the following regimens with individual patient-based modifications, including (a) 60 mg/m2 of doxorubicin (anthracycline) for 4 cycles, cyclophosphamide and taxol or (b) 8 mg/kg loading + 6 mg/kg trastuzumab, taxol, carboplatin with/without pertuzumab. Of the eleven patients, seven had undergone the anthracycline treatment and four had undergone the trastuzumab treatment. Additionally, full LV short-axis data with SSFP (Steady State Free Precession) were acquired in the patients to validate their LVEF measurements. DENSE acquisitions in N=11 healthy female subjects (without existing heart failure or related comorbidities) contributed to a 1:1 age-matched comparison of contractile parameters with subjects either newly recruited or their data taken from an existing database [28-31, 33].

B. DENSE Acquisition and Protocols

Navigator-gated, spiral 3D DENSE data were acquired with displacement encoding applied in two orthogonal in-plane directions and one through plane direction [23, 24, 27, 30]. A flexible, anterior 6-channel body matrix RF coil (Siemens Healthcare, Erlanger, Germany) and the table-mounted spine matrix RF coil were used for receiving signals. Typical imaging parameters included field of view (FOV) of 380×380 mm^2, echo time (TE)

of 1.04 ms, repetition time (TR) of 15 ms, flip angle (FA) of 20°, matrix size of $128 \times 128 \times 19$, $2.97 \times 2.97 \times 5$ mm^3 voxel size, 21 cardiac phases, encoding frequency of 0.06 cycles/mm, simple 4-point encoding and 3-point phase cycling for artifact suppression [26, 27]. The number of navigator-accepted heartbeats to complete a single partition in 3D is 36 heartbeats given that three are needed to acquire a complete set of spirals for a single displacement encoding direction and a single phase cycling point [27]. SSFP acquisition consisted of a FOV of 340×276 mm^2, TE of 1.48 ms, TR of 51.15 ms, FA of 80°, matrix size of $192 \times 156 \times 12$, 1.77×1.77 mm^2 pixel size, slice thickness of 7mm and 25 cardiac phases. Continuous monitoring of heart rates (HR) and blood pressures (BP) was conducted for all patient scans.

C. Automated Boundary Detection

As outlined in our previous publication this automated process consists of identifying the left-ventricular boundary contours in the most basal short-axis slice at end-diastole with the operator selecting an ellipsoidal region of interest (ROI), and followed by propagating the boundaries to all short axis slice positions between end-diastole and end-systole, as well as base to apex [31-33]. The LV boundaries and intramural tissue are identified using Otsu's Method which is a non-uniform quantization scheme based on image histogram bins that yields a threshold-based image with a distinct profile of the short-axis [31-33]. Additionally, this study is unique in combining the unwrapped displacement vectors toward precisely tracking and relocating a boundary point between end-diastole and end-systole. Following is the generation of boundaries for all partitions and timeframes using the above technique as well as the reconstructing of 3D LV. Chamber quantifications included measuring chamber diameters, end-diastolic volume (EDV), end-systolic volume (ESV), stroke volume (SV) and LVEF [31-33].

D. Automated Strain Analysis with Radial Point Interpolation Method

Three-dimensional strain tensors were computed using RPIM at each voxel in the patient's reconstructed 3D geometries. RPIM is a numerical analysis technique based on the Galerkin weak form that uses radial basis functions (RBF) as shape functions, which facilitates fast multidimensional computations of strain. Extensive descriptions of computing 3D LV strains with RPIM and by using Multiquadrics (MQ) as RBF shape function are outlined in our previous literature [29, 30, 33-36]. The LV torsion definition used was the relative angle of twist between basal and apical rotations, and given by [20],

$$\alpha_T = \frac{(\varphi_{base} - \varphi_{apex})(\rho_{base} + \rho_{apex})}{2D} \qquad (1)$$

where φ is the angle of twist, ρ is the radius, and D is the inter-segment distance. Using the above methodologies for boundary detection and strain analysis, contractile parameters between the patients and healthy subjects were compared and significant differences in strains, torsion and chamber dimensions observed.

E. Statistical Analysis

The results of chamber quantification from the DENSE magnitude images were compared to those from the SSFP acquired on the same day via paired t-test analysis, and to their latest obtained transthoracic echocardiogram (TTE) following their chemotherapy examinations. The methodology for analyzing strain in this study has been previously validated, to increase confidence in the analysis, interobserver measurements of the patients' strains were conducted by independent users and agreement established with the Bland-Altman method. All contractile parameters in patients were compared to those in our healthy subjects' database to observe changes due to remodeling with homoscedastic two-sample t-tests.

III. RESULTS

The average age of the patients was 56.8 ± 8.9 years and body mass was 72.9 ± 20.2 kilograms. Monitored mean heart rate (HR) was 82.0 ± 18.6 bpm while mean blood pressure (BP) was $126.8 \pm 21.7/78.3 \pm 12.8$ mmHg. The average age of the healthy subjects was 54.5 ± 6.6 years and body mass was 71.7 ± 9.8 kilograms, monitored mean heart rate (HR) was 72.1 ± 9.8 bpm and mean blood pressure (BP) was $123.8 \pm 14.1/69.9 \pm 7.8$ mmHg. LV chamber dimensions and quantities are given in Table 1 and the strain-based contractile parameters in Table 2. Results from comparisons of LVEF measured with DENSE and SSFP were 0.52 ± 0.11 vs 0.48 ± 0.15 (p=0.33), 0.55 ± 0.09 vs 0.54 ± 0.12 (p=0.19), and 0.52 ± 0.12 vs 0.54 ± 0.11 (p=0.60) for the basal, mid-ventricular and apical segments, respectively. Results from comparing DENSE versus TTE LVEF were 0.52 ± 0.10 vs 0.54 ± 0.17 (p=0.35) for the whole LV. Fig. 1 shows the typical differences in DENSE based 3D displacements that could be observed between patients and healthy subjects.

Fig. 2 and Fig. 3 shows the 3D surface strain maps in the entire LV for torsion and longitudinal in a single patient and a single healthy subject that is typically representative of the population-based differences given in Table 2.

Table 1. Systolic Chamber Quantifications

Parameter	Patient	Healthy	p-value
Diameter B (D) (cm)	6.0 ± 1.1	5.2 ± 1.0	0.03*
Diameter M (D) (cm)	5.2 ± 1.2	5.1 ± 1.3	0.70
Diameter A (D) (cm)	3.5 ± 1.2	3.5 ± 0.8	0.90
Diameter B (S) (cm)	4.3 ± 1.1	3.4 ± 0.8	0.03*
Diameter M (S) (cm)	3.5 ± 1.2	3.2 ± 0.7	0.40
Diameter A (S) (cm)	2.2 ± 1.2	2.1 ± 0.9	0.60
EF B (%)	47 ± 12	61 ± 9	0.01*
EF M (%)	56 ± 11	61 ± 6	0.10
EF A (%)	60 ± 8	63 ± 8	0.30
EF Full LV	55 ± 15	62 ± 7	0.10
SV B (cm³)	39.9 ± 8.1	44.4 ± 10.6	0.40
SV M (cm³)	24.8 ± 8.0	29.1 ± 11.3	0.30
SV A (cm³)	16.9 ± 5.5	21.0 ± 7.0	0.30

Abbreviations: D: diastolic, S: systolic, B: basal, M: mid-ventricular, A: Apical, EF: ejection fraction SV: stroke volume. *Indicates significant differences between patients and healthy subjects.

Table 2. Systolic Strains and Torsional Parameters

Strain	Patient	Healthy	P-value
E_{cc} Basal	-0.17 ± 0.04	-0.20 ± 0.05	0.30
E_{cc} Mid	-0.21 ± 0.03	-0.22 ± 0.04	0.90
E_{cc} Apical	-0.21 ± 0.03	-0.24 ± 0.03	0.10
E_{ll} Basal	-0.14 ± 0.03	-0.19 ± 0.03	0.04*
E_{ll} Mid	-0.15 ± 0.03	-0.21 ± 0.05	0.04*
E_{ll} Apical	-0.17 ± 0.02	-0.22 ± 0.05	0.02*
E_{rr} Basal	0.37 ± 0.09	0.34 ± 0.03	0.22
E_{rr} Mid	0.28 ± 0.06	0.32 ± 0.03	0.20
E_{rr} Apical	0.23 ± 0.04	0.30 ± 0.03	0.01*
Rotation Bas (°)	-1.76 ± 1.13	-5.51 ± 2.17	0.00**
Rotation Mid (°)	5.27 ± 2.20	7.30 ± 2.68	0.00**
Rotation Apex (°)	8.62 ± 3.93	14.59 ± 3.88	0.00**
Torsion Bas (°)	-	-	-
Torsion Mid (°)	5.47 ± 1.79	8.80 ± 1.68	0.02*
Torsion Apical (°)	6.20 ± 1.93	10.64 ± 1.58	0.00**

Abbreviations: rr: radial, cc: circumferential, ll: longitudinal. *Indicates significant differences between patients and healthy subjects. **Indicates p<0.001.
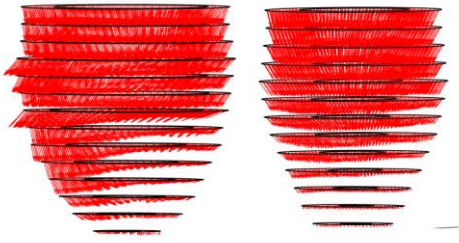
Figure 1. Phase unwrapping based 3D displacement vectors computed in the full LV of a patient (Left) and a healthy subject (Right).
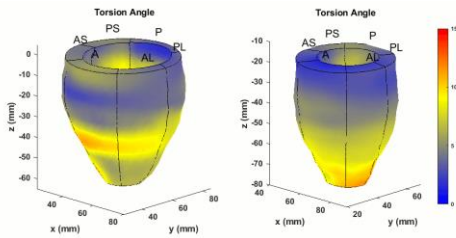
Figure 2. Three-dimensional torsional strain maps generated with the automated strain analysis algorithm in the full LV of a patient (Left) and a healthy subject (Right).
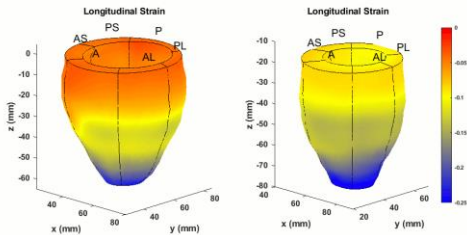
Figure 3. Three-dimensional longitudinal strain maps generated with the automated strain analysis algorithm in the full LV of a patient (Left) and a healthy subject (Right).

IV. DISCUSSION

To begin, the chamber quantities measured in healthy subjects (Table 1), including parameters such as CD, EDV, ESV and EF, are comparable to values found in our semi-automated validation study and in others [31, 37]. Similar observations can be made regarding the strains in healthy subjects given in Table 2 against those observed in our previous validation studies and others [31, 37, 38]. The shear strain results in healthy subjects in Table 2 are comparable to those found in previous literature and very similar to the Young et al. study which reported 0.01-0.03 for apical, 0.03-0.04 for mid-ventricular, and 0.03-0.04 for basal region E_{cl}, which is the strain most closely related to the mechanics of LV torsion [39].

Discussed next is the LV remodeling predicted with this algorithm and differences in chamber quantifications and strains between patients and healthy subjects as shown in Tables 1 and 2. Of particular interest is a study by Siedman et al., which shows the imminent manifestation of systolic abnormalities when patients were administered a combined dose of CAs including anthracyclines, trastuzumab, and cyclophosphamides, as was seen in this study [40]. Studies also show that myocardial dysfunction measured with global and regional computations of 3D strains (and torsion) are more sensitive toward detection of cardiotoxicity prior to any significant LVEF indications. Very little literature is available in regards to altered chamber diameters in breast cancer survivors or in relation to cardiotoxicity remodeling, with the Motoki et al. study being one that did report a diameter of 2.8 ± 0.5 cm versus the 2.2 ± 0.6 cm (mid-ventricular) found in this study [11]. While the reduced peak systolic normal strains and torsion in Table 2 have been shown in breast cancer (cardiotoxicity) patients in previous studies, no data regarding the peak systolic shear strains can be found in literature [4, 9-12, 16]. Particular differences can be seen in strain parameters versus the healthy database, such as longitudinal strains and torsion, which has also been reported as changed significantly in previous studies [2, 11, 13, 16, 18, 41, 42]. In this respect, the ability to detect any impaired functionality (cardiotoxicity) in the LV with strain parameters similar to our study was shown previously by two others, one by Sawaya et al. who showed a decline in longitudinal strain following treatment with anthracyclines, trastuzumab and taxanes and the other by Motoki et al. who showed declined torsion in patients treated with anthracyclines [11, 16]. After showing a significant negative correlation between cumulative anthracycline doses and torsion, Motoki et al. emphasized that torsional deformation is obvious due to cardiotoxicity affecting the helically oriented myocardial fibers. A number of studies in other LV impairments have also shown primary altered patterns in torsion due to adverse effects on fiber orientation, an example of which is the divergent rotation patterns in the same direction at all levels in dilated cardiomyopathy [20]. While previous studies show measurements of reduced peak systolic longitudinal strain between 9% and 19% and peak systolic torsion ranging 6% to 17% in a way similar to this study, this study did not find a reduction in peak systolic radial strain as high as 40% or peak systolic circumferential strain of 11% to 16.7% reported previously [9-12, 16, 17]. In relation to the surface strain maps that are generated in Fig. 2, it can be said to be similar to T1/T2 or contrast mapping that show the diffuse myocardial fibrosis (DMF) in cardiotoxicity [6]. Within our recent case-study where cardiotoxicity was first indicated by lower torsion and longitudinal strain in a 54 year old female chemotherapy patient treated with

Adriamycin, cyclophosphamide and Herceptin and who later received Ado–Trastuzumab Emtansine but her LVEF was at 48% [43]. Following the strain-based findings, a TTE reexamination after two-months showed a drop in LVEF to < 25% which meant >10% drop between subsequent tests that conform to GDMT-based diagnosis of cardiotoxicity in breast cancer patients. Her case is excluded from this study due to the existence of acute cardiac complications and her very low ejection fraction. Other studies show reduced peak systolic longitudinal strain between 9% and 19% and torsional reductions as high as 50%. This effect is seen in this study with the reduced peak longitudinal strains and torsion, which is not seen via LVEF reductions (Table 2) [9, 11].

The first limitation of this study is in not providing a strong validation for reporting the patients' shear strains. Secondly this study is not a longitudinal study where the exact extent of remodeling in the patients LVs are tracked and reported. Hence any scientific basis of confirming cardiotoxicity despite differences found in the patients' contractile parameters could not be established. It is further limited by the mean patient LVEF lying at the borderline of normal according to GDMT guidelines and significant differences not seen versus the healthy subjects' database. A third limitation is that any strain differences in the patients' strains were not adjusted according to other existing cardiac co-morbidities.

V. CONCLUSION

This study shows that cardiac remodeling following treatment with anthracycline and trastuzumab types of CAs can be detected with fast, inexpensive and automated strain mapping, which is a metric capable of detecting altered material properties and function. However, the thresholds of strain that define myocardial dysfunction related to cardiotoxicity will require a clinical study before this metric is used as a diagnostic tool.

ACKNOWLEDGMENTS

REFERENCES

[1] D. Cardinale, A. Colombo, G. Lamantia, N. Colombo, M. Civelli, G. De Giacomi, M. Rubino, F. Veglia, C. Fiorentini, and C.M. Cipolla, "Anthracycline-induced cardiomyopathy: clinical relevance and response to pharmacologic therapy", *Journal of the American College of Cardiology*, 2010, 55, (3), pp. 213-220

[2] R. Jurcut, H. Wildiers, J. Ganame, J. D'Hooge, R. Paridaens, and J.U Voigt, "Detection and monitoring of cardiotoxicity-what does modern cardiology offer?", *Support Care Cancer*, 2008, 16, (5), pp. 437-445

[3] M.G. Khouri, P.S. Douglas, J.R. Mackey, M. Martin, J.M. Scott, M. Scherrer-Crosbie, and L.W Jones, "Cancer therapy-induced cardiac toxicity in early breast cancer: addressing the unresolved issues", *Circulation*, 2012, 126, (23), pp. 2749-2763

[4] P. Stoodley, D. Tanous, D. Richards, S. Meikle, J. Clarke, R. Hui, and L. Thomas, "Trastuzumab-induced cardiotoxicity: the role of two-dimensional myocardial strain imaging in diagnosis and management", *Echocardiography*, 2012, 29, (6), pp. E137-140

[5] J.L. Hare, J.K. Brown, R. Leano, C. Jenkins, N. Woodward, and T.H. Marwick, "Use of myocardial deformation imaging to detect preclinical myocardial dysfunction before conventional measures in patients undergoing breast cancer treatment with trastuzumab", *American Heart Journal*, 2009, 158, (2), pp. 294-301

[6] J.H. Jordan, et. al., "Anthracycline-Associated T1 Mapping Characteristics Are Elevated Independent of the Presence of Cardiovascular Comorbidities in Cancer Survivors", *Circ Cardiovasc Imaging*, 2016, 9, (8)

[7] Hunt, S.A., et al., "ACC/AHA 2005 Guideline Update for the Diagnosis and Management of Chronic Heart Failure in the Adult: a report of the American College of Cardiology/American Heart Association Task Force on Practice Guidelines (Writing Committee to Update the 2001 Guidelines for the Evaluation and Management of Heart Failure): developed in collaboration with the American College of Chest Physicians and the International Society for Heart and Lung Transplantation: endorsed by the Heart Rhythm Society", *Circulation*, 2005, 112, (12), pp. e154-235

[8] D. Slamon, et al., "Adjuvant trastuzumab in HER2-positive breast cancer", *N Engl J Med*, 2011, 365, (14), pp. 1273-1283

[9] P. Thavendiranathan, F. Poulin, K.D. Lim, J.C. Plana, A. Woo, and T.H. Marwick, "Use of myocardial strain imaging by echocardiography for the early detection of cardiotoxicity in patients during and after cancer chemotherapy: a systematic review", *Journal of the American College of Cardiology*, 2014, 63, (25 Pt A), pp. 2751-2768

[10] H. Sawaya, et al., "Early detection and prediction of cardiotoxicity in chemotherapy-treated patients", *The American Journal of Cardiology*, 2011, 107, (9), pp. 1375-1380

[11] H. Motoki, J. Koyama, H. Nakazawa, K. Aizawa, H. Kasai, A. Izawa, T. Tomita, Y. Miyashita, S. Kumazaki, M. Takahashi, and U. Ikeda, "Torsion analysis in the early detection of anthracycline-mediated cardiomyopathy", *Eur Heart J Cardiovasc Imaging*, 2012, 13, (1), pp. 95-103

[12] C. Mornos, and L. Petrescu, "Early detection of anthracycline-mediated cardiotoxicity: the value of considering both global longitudinal left ventricular strain and twist", *Can J Physiol Pharmacol*, 2013, 91, (8), pp. 601-607

[13] R. Jurcut, H. Wildiers, J. Ganame, J. D'Hooge, J. De Backer, H. Denys, R. Paridaens, F. Rademakers, and J.U. Voigt, "Strain rate imaging detects early cardiac effects of pegylated liposomal Doxorubicin as adjuvant therapy in elderly patients with breast cancer", *Journal of the American Society of Echocardiography : official publication of the American Society of Echocardiography*, 2008, 21, (12), pp. 1283-1289

[14] L.W. Jones, M.J. Haykowsky, J.J. Swartz, P.S. Douglas, and J.R. Mackey, "Early breast cancer therapy and cardiovascular injury", *Journal of the American College of Cardiology*, 2007, 50, (15), pp. 1435-1441

[15] D. Cardinale, A. Colombo, G. Bacchiani, I. Tedeschi, C.A. Meroni, F. Veglia, M. Civelli, G. Lamantia, N. Colombo, G. Curigliano, C. Fiorentini, and C.M. Cipolla, "Early detection of anthracycline cardiotoxicity and improvement with heart failure therapy", *Circulation*, 2015, 131, (22), pp. 1981-1988

[16] H. Sawaya, et al., "Assessment of echocardiography and biomarkers for the extended prediction of cardiotoxicity in patients treated with anthracyclines, taxanes, and trastuzumab", *Circ Cardiovasc Imaging*, 2012, 5, (5), pp. 596-603

[17] P.W. Stoodley, D.A. Richards, R. Hui, A. Boyd, P.R. Harnett, S.R. Meikle, J. Clarke, and L. Thomas, "Two-dimensional myocardial strain imaging detects changes in left ventricular systolic function immediately after anthracycline chemotherapy", *Eur J Echocardiogr*, 2011, 12, (12), pp. 945-952

[18] J.T. Poterucha, S. Kutty, R.K. Lindquist, L. Li, and B.W. Eidem, "Changes in left ventricular longitudinal strain with anthracycline chemotherapy in adolescents precede subsequent decreased left ventricular ejection fraction", *Journal of the American Society of Echocardiography : official publication of the American Society of Echocardiography*, 2012, 25, (7), pp. 733-740

[19] J.V. McGowan, R. Chung, A. Maulik, I. Piotrowska, J.M. Walker, and D.M. Yellon, "Anthracycline Chemotherapy and Cardiotoxicity", *Cardiovasc Drugs Ther*, 2017, 31, (1), pp. 63-75

[20] P.P. Sengupta, A.J. Tajik, K. Chandrasekaran, and B.K. Khandheria, "Twist mechanics of the left ventricle: principles and application", *JACC Cardiovasc Imaging*, 2008, 1, (3), pp. 366-376

[21] I.K. Russel, M.J. Gotte, J.G. Bronzwaer, P. Knaapen, W.J. Paulus, and A.C. van Rossum, "Left ventricular torsion: an expanding role in the analysis of myocardial dysfunction", *JACC Cardiovasc Imaging*, 2009, 2, (5), pp. 648-655

[22] Y. Notomi, P. Lysyansky, R.M. Setser, T. Shiota, Z.B. Popovic, M.G. Martin-Miklovic, J.A. Weaver, S.J. Oryszak, N.L. Greenberg, R.D. White, and J.D. Thomas, "Measurement of ventricular torsion by two-dimensional ultrasound speckle tracking imaging", *Journal of the American College of Cardiology*, 2005, 45, (12), pp. 2034-2041

[23] D. Kim, W.D. Gilson, C.M. Kramer, and F.H. Epstein, "Myocardial tissue tracking with two-dimensional cine displacement-encoded MR imaging: development and initial evaluation", *Radiology*, 2004, 230, (3), pp. 862-871

[24] B.S. Spottiswoode, X. Zhong, A.T. Hess, C.M. Kramer, E.M. Meintjes, B.M. Mayosi, and F.H. Epstein, "Tracking myocardial motion from cine DENSE images using spatiotemporal phase unwrapping and temporal fitting", *IEEE Transactions on Medical Imaging*, 2007, 26, (1), pp. 15-30

[25] A.H. Aletras, S. Ding, R.S. Balaban, and H. Wen, "DENSE: displacement encoding with stimulated echoes in cardiac functional MRI", *J Magn Reson*, 1999, 137, (1), pp. 247-252

[26] X. Zhong, L.B. Gibberman, B.S. Spottiswoode, A.D. Gilliam, C.H. Meyer, B.A. French, and F.H. Epstein, "Comprehensive cardiovascular magnetic resonance of myocardial mechanics in mice using three-dimensional cine DENSE", *Journal of Cardiovascular Magnetic Resonance : Official Journal of the Society for Cardiovascular Magnetic Resonance*, 2011, 13, pp. 83

[27] X. Zhong, B.S Spottiswoode, C.H. Meyer, C.M. Kramer, and F.H. Epstein, "Imaging three-dimensional myocardial mechanics using navigator-gated volumetric spiral cine DENSE MRI", *Magnetic Resonance in Medicine : official journal of the Society of Magnetic Resonance in Medicine / Society of Magnetic Resonance in Medicine*, 2010, 64, (4), pp. 1089-1097

[28] J. Kar, B. Cupps, X. Zhong, D. Koerner, K. Kulshrestha, S. Neudecker, J. Bell, H. Craddock, and M. Pasque, "Preliminary investigation of multiparametric strain Z-score (MPZS) computation using displacement encoding with simulated echoes (DENSE) and radial point interpretation method (RPIM)", *Journal of Magnetic Resonance Imaging : JMRI*, 2016, 44, (4), pp. 993-1002

[29] J. Kar, A.K. Knutsen, B.P. Cupps, and M.K. Pasque, "A validation of two-dimensional in vivo regional strain computed from displacement encoding with stimulated echoes (DENSE), in reference to tagged magnetic resonance imaging and studies in repeatability", *Annals of Biomedical Engineering*, 2014, 42, (3), pp. 541-554

[30] J. Kar, A.K. Knutsen, B.P. Cupps, X. Zhong, and M.K. Pasque, "Three-dimensional regional strain computation method with displacement encoding with stimulated echoes (DENSE) in non-ischemic, non-valvular dilated cardiomyopathy patients and healthy subjects validated by tagged MRI", *Journal of Magnetic Resonance Imaging : JMRI*, 2015, 41, (2), pp. 386-396

[31] J. Kar, X. Zhong, M.V. Cohen, D.A. Cornejo, A. Yates-Judice, E. Rel, and M.S. Figarola, "Introduction to a mechanism for automated myocardium boundary detection with displacement encoding with stimulated echoes (DENSE)", *Br J Radiol*, 2018, pp. 20170841

[32] Kar, J.C., B.P.; Pasque, M.K.: 'Systems and methods for measuring cardiac strain', 2018-05-03 2018

[33] G. Angus-Barker and J. Kar, "Comprehensive Fully Automated Left-Ventricular Ejection and Contractility Analysis" (2018.2018)

[34] G.R Liu, "Meshfree Methods: Moving Beyond the Finite Element Method", (CRC Press, 2009, 2 edn. 2009)

[35] J.G. Wang, and G.R. Liu, "A point interpolation meshless method based on radial basis functions.", *Int J Numer Methods Eng,* 2002, 54, pp. 1623-1648

[36] J.G. Wang, and G.R. Liu, "On the optimal shape parameters of radial basis functions used for 2-D meshlesss methods.", *Computer Methods in Applied Mechanics and Engineering,* 2002, 191, (23-24), pp. 2611-2630

[37] L.E. Hudsmith, S.E. Petersen, J.M. Francis, M.D. Robson, and S. Neubauer, "Normal human left and right ventricular and left atrial dimensions using steady state free precession magnetic resonance imaging", *Journal of Cardiovascular Magnetic Resonance : Official Journal of the Society for Cardiovascular Magnetic Resonance*, 2005, 7, (5), pp. 775-782

[38] M.J. Gotte, T. Germans, I.K. Russel, J.J. Zwanenburg, J.T. Marcus, A.C. van Rossum, and D.J. van Veldhuisen, "Myocardial strain and torsion quantified by cardiovascular magnetic resonance tissue tagging: studies in normal and impaired left ventricular function", *Journal of the American College of Cardiology*, 2006, 48, (10), pp. 2002-2011

[39] A.A. Young, C.M. Kramer, V.A. Ferrari, L. Axel, and N. Reichek, "Three-dimensional left ventricular deformation in hypertrophic cardiomyopathy", *Circulation*, 1994, 90, (2), pp. 854-867

[40] A. Seidman, C. Hudis, M.K. Pierri, S. Shak, V. Paton, M. Ashby, M. Murphy, S.J. Stewart, and D. Keefe, "Cardiac dysfunction in the trastuzumab clinical trials experience", *J Clin Oncol*, 2002, 20, (5), pp. 1215-1221

[41] M.C. Pinder, Z. Duan, J.S. Goodwin, G.N. Hortobagyi, and S.H. Giordano, "Congestive heart failure in older women treated with adjuvant anthracycline chemotherapy for breast cancer", *J Clin Oncol*, 2007, 25, (25), pp. 3808-3815

[42] T.C. Tan, and M. Scherrer-Crosbie, "Cardiac complications of chemotherapy: role of imaging", *Curr Treat Options Cardiovasc Med*, 2014, 16, (4), pp. 296

[43] J. Kar, B.M. Baldwin, M.K. Cohen, S. Joseph, A. Chowdry, M.S. Figarola, C.M. Malozzi, "A Case-Study in MRI-based Automated Detection of Left-ventricular Cardiotoxicity in a Breast Cancer Patient after Chemotherapy Treatment", in Editor (Ed.)^(Eds.): 'Book A Case-Study in MRI-based Automated Detection of Left-ventricular Cardiotoxicity in a Breast Cancer Patient after Chemotherapy Treatment' (SCMR, 2019, edn.), pp.